Structural Development and Adhesion of Acrylic ABA Triblock Copolymer Gels

Cynthia M. Flanigan, Alfred J. Crosby, and Kenneth R. Shull*

Department of Materials Science and Engineering, Northwestern University, Evanston, Illinois 60208

Received June 2, 1999; Revised Manuscript Received August 3, 1999

ABSTRACT: Relationships between the structure, properties, and processing techniques of model polymer gels are investigated. The mechanical properties of the gels are determined by a thermally reversible aggregation of the syndiotactic PMMA end blocks of an acrylic triblock copolymer, which is diluted with a selective solvent for the center block. The adhesive and mechanical properties of these gels are related to their structural features, which are quantified by small-angle X-ray scattering experiments. The gels are significantly strengthened by the addition of low molecular weight isotactic PMMA homopolymers. These polymers form complexes with the syndiotactic PMMA end blocks of the triblock copolymer. In addition, we employ an axisymmetric adhesion test to demonstrate that the equilibrium gelation process can be utilized to reproducibly control the structure and adhesive properties of "dried" polymers. Acrylic acid moieties increase the adhesive performance of these materials without affecting their structure. By employing a unique gel casting process, a network structure with the desired properties can be formed, giving materials that are ideally suited for use as pressure-sensitive adhesives.

Introduction

Interest in self-organizing polymer gels has expanded over the past several years as investigators have recognized the ability to develop processing routes that yield materials with very well controlled structures and properties. Extensive studies have been conducted on the structural morphologies of ABA type triblock copolymer gels, using small-angle X-ray scattering and small-angle neutron scattering[1−5] in addition to other techniques.[6−10] Many of these reports have focused on the microphase separation of block copolymers with glassy end blocks and a rubbery midblock.[4,5] Kleppinger et al. have studied the effects of temperature and overall polymer concentration on the stability of glassy domains obtained from ordered triblock copolymer/solvent mixtures, where the solvent preferentially dissolves the midblock.[11] Dependencies of the gel's morphology on the copolymer concentration, temperature, and bulk deformation have been described in detail.[2,3,10,12,13] Some of these discussions have related the gel's structural features either to its mechanical behavior or to the effect of different processing routes on its final microstructure. Laurer et al., for example, have researched the effects of polymer concentration and processing schemes on the behavior and morphology of a commercial elastomer gel comprised of polystyrene end blocks and a ethylene-*co*-butylene midblock.[10]

Clearly, the interplay between processing, microstructure, and properties is an important engineering and scientific concern. Recent works on commercial thermoplastic elastomer gels and physically weak hydrogel materials have concentrated on microstructural studies as they relate to either processing routes or, in some cases, bulk mechanical properties.[10,11,13] While current studies provide insight as to the processing/structure or mechanical properties/structure relationships, there remains a fundamental question of interest: how do processing techniques affect both the gel's structural properties and its adhesive characteristics?

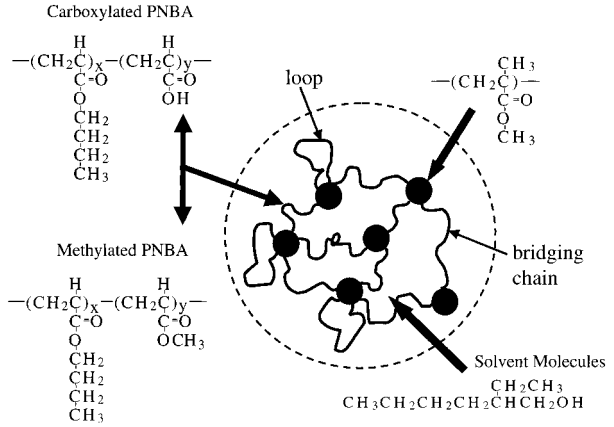

Figure 1. Microstructural representation of a gel layer, formed by diluting a PMMA−PNBA−PMMA triblock copolymer with a selective solvent for the center block. The PNBA can form either "loop" or "bridging chain" configurations. The structures of the carboxylated and methylated midblock are illustrated as well, in which "*y*" constitutes only a few mole percent of acrylic acid or methyl moieties within the copolymer.

To our knowledge, employing gel processing techniques to control the morphology of polymers obtained after solvent removal has generally been overlooked. In pressure-sensitive adhesive (PSAs) applications, for example, developing a controlled morphology is critical for the reproducibility of the product.

In our work, we examine the relationships between the structural network formation, adhesive properties, and processing routes of a well-characterized model gel system. A triblock copolymer with glassy end blocks of poly(methyl methacrylate) (PMMA) and rubbery midblock of poly(*n*-butyl acrylate) is diluted with a preferential solvent for the midblock, to form a gel that behaves as an elastic solid at room temperature. Advantages of these polyacrylate gels include their reversible transition to a liquid state at relatively low temperatures (∼65 °C) in addition to their strength and remarkable elasticity at room temperature. The schematic in Figure 1 illustrates the three-dimensional

* To whom correspondence should be addressed.

10.1021/ma990873h CCC: $18.00
Published on Web 09/28/1999

network that forms from the triblock copolymer swollen with a selective solvent for the middle block. The PMMA chains aggregate into domains, as depicted by the filled circles, and are interconnected with the PNBA chains that span through the solvent matrix. For the diblock/triblock blends, the three possible orientations of the rubbery block chains are loop structures, dangling ends, and interconnecting strands between domains. These configurations have a direct impact on the elasticity and mechanical properties of the gel since the ratio of bridging chains to either loops or dangling ends dominates the elastic nature of the material. Also, the concentration of polymer within the gel impacts the formation of the network by influencing the fraction of bridging molecules and size of PMMA domains.

In this paper, we demonstrate that the equilibrium gelation process can be utilized to reproducibly control the structure of "dried" polymers. We compare the adhesive response of polymers processed by a gel casting technique to those processed by a solution casting technique, where the solvent is not preferential for either the A or B blocks. During gel processing, the polymer chains retain their overall microstructural configuration even as solvent is removed. We also use small-angle X-ray scattering (SAXS) experiments to investigate the effects of temperature and polymer concentration on structural features such as the spacing between the glassy PMMA domains. In addition, we explore the effects of stereocomplexation of low molecular weight isotactic PMMA chains with the glassy domains within the gel. These homopolymer chains strengthen the gel network by forming complexes with the syndiotactic end blocks of the triblock copolymer.[14] Last, we examine the effects of acrylic acid moieties on the structural development of the polymer network. Other studies have indicated that small amounts of acrylic acid groups (3−4 mol %) within the polymer or copolymer will greatly enhance its adhesive properties.[15−18] We probe these effects by performing axisymmetric adhesion tests on thin, polymer layers using a glass, hemispherical indenter.

Experimental Section

Materials. Physically cross-linked polymer gels were formed by diluting a poly(methyl methacrylate)−poly(*n*-butyl acrylate)−poly(methyl methacrylate) triblock copolymer with either 2-ethylhexanol or 3,7-dimethyl-1-octanol, which are both preferential solvents for the middle block. The synthesis of the polyacrylate copolymers used here has been discussed previously[19,20] and is based upon the anionic polymerization techniques of Varshney et al.[21] Gels have been formed from two different versions of this copolymer: Triblock 1 (T1) and diblock−triblock 1 (D/T1). The T1 polymer has a total molecular weight of 138 000 g/mol (67 wt % PNBA) with a polydispersity index of 1.1. The D/T1 polymer, a blend of diblock and triblock chains, has a molecular weight of 167 000 g/mol (82 wt % PNBA), with a polydispersity index of 1.12. During the synthesis of the D/T1 copolymer, some of the reactive sites on the difunctional initiator were terminated, leading to a blend formation of triblock and diblock chains. The weight fraction of these diblock chains in the D/T1 copolymer is approximately 0.35. As discussed in a recent paper, PNBA blocks of these polymers contain a few mole percent of acrylic acid moieties introduced during the acid-catalyzed transalcoholysis of the parent poly(*tert*-butyl acrylate) block.[22] We chemically converted this "carboxylated" polyacrylate with diazomethane in order to replace the acrylic acid functional groups with methyl groups, based upon reported procedures.[23] The details of this reaction for a poly(*n*-butyl acrylate) homopolymer are described by Ahn and Shull.[15] Through this conversion process, we formed a methylated version of the T1 triblock copolymer. Figure 1 shows the polymer structure of the carboxylated and methylated forms, where $x \gg y$.

For the SAXS experiments, we prepared a range of different polymer gels including D/T1 gels with 5, 15, and 25 vol % polymer and T1 carboxylated and methylated gels with 5 and 14 vol % polymer. Solutions based upon the D/T1 and T1 polymers were formed at elevated temperatures of ∼65 °C and were cooled to room temperature to form physically cross-linked networks. In addition, we investigated the effects of stereocomplexation of the syndiotactic PMMA domains with a low molecular weight isotactic PMMA polymer by forming D/T1 gels with 5 and 25 vol % polymer. The PMMA homopolymer, with a molecular weight of 10 000 g/mol, was obtained from Polysciences and was blended with the polymer solution at elevated temperatures to form a well-dispersed blend in the liquidlike state. The polymer solution was cooled to room temperature to form a solid, elastic gel. The originally transparent gels became bluish-white upon addition of the isotactic PMMA. On the basis of the molecular weights of the chains, a ratio of 0.5 of isotactic PMMA to syndiotactic PMMA was used to determine the appropriate amount of homopolymer. Yu and Jerome showed that stereocomplexes were optimally formed under these conditions.[14]

Methods. The SAXS experiments were conducted at the Advanced Photon Source at Argonne National Laboratories. Gel samples with thickness of ∼1 mm were sealed in 3 cm diameter Kapton disks and placed within a hot stage with center slit. An external temperature controller allowed in situ heating and cooling of the samples from room temperature to 100 °C, as scattering patterns were recorded in intervals of 3 or 4 min. A range of q ($q = 4\pi \sin \theta/\lambda$) values from 0.08 to 1.1 nm^{-1} was covered, using 7.5 keV X-rays ($\lambda = 0.165$ nm.) We employed a two-dimensional X-ray detector to record the scattering patterns and an azimuthal scan to extract a one-dimensional set of data from each run.

Our methods for determining the adhesive and mechanical properties of the gels have been described elsewhere.[20,22] Briefly, a VOR Bohlin rheometer with couette geometry was used to measure the time- and frequency-dependent shear response of the D/T iPMMA gels after they are cooled from elevated temperatures to room temperature. The dynamic moduli, G' and G'', were measured over a temperature range from 25 to 80 °C. For the "dried" gels, we employed an axisymmetric adhesion test and linear elastic fracture mechanics to quantify the adhesion between a rigid indenter and a thin polymer layer.[24] For our experiments, an optically smooth, hemispherical indenter, with diameter 12 mm, was pressed into a polyacrylate layer, with typical thickness between 60 and 280 μm. This adhesive layer was prepared by two different techniques: solution casting and gel casting. For the solution casting method, the D/T1 copolymer was dissolved in toluene, a good solvent for both the PMMA end blocks and the PNBA midblock. This polymer solution was cast onto a glass slide using a doctor-blading technique and dried at low temperatures for 3 days. Upon removal of the solvent, the layer's thickness was measured using a displacement sensor with 1 μm accuracy. For the gel casting processing route, the polyacrylate gel was heated between a fluorinated glass slide and a nontreated slide, which were separated by rigid shims of a known thickness. At temperatures above the gel point, the gel was able to flow between the two surfaces to form a uniform layer. The gel layer was cooled to room temperature, at which point the fluorinated surface was removed easily from the elastic layer. The alcohol was evaporated from the gel at a temperature below the gel point, leaving a polyacrylate film on the glass slide.

During the adhesion tests, the rigid indenter was pressed into the adhesive layer and retracted, as simultaneous measurements of the applied load, contact area, and displacement were recorded. Figure 2 shows this testing geometry in which a 12 mm diameter glass hemisphere is pressed into the polymer layer up to a predetermined load. The load and displacement between the two contacting surfaces were directly acquired, using a 50 g load cell and a displacement

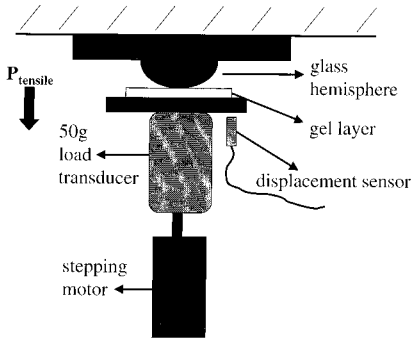

Figure 2. Schematic of adhesion test geometry for a 12 mm diameter hemispherical, glass indenter in contact with a "dried" gel layer. The 50 g load transducer and displacement sensor are used to simultaneously record the applied load and displacement between the fixed probe and mobile adhesive layer. The arrow indicates the direction of the positive tensile forces.

sensor, respectively. A camera, optical microscope, and video cassette recorder were used to measure the maximum contact area for each test. Using a LabView computer program, the stepping motor was controlled precisely so that the rigid indenter was pressed into the adhesive layer until a maximum compressive load of 25 mN was reached. At this point, the motor was retracted until the adhesive debonded from the indenter's surface. Tack curves, representing the load−displacement relationship, were obtained for each adhesive using this method. For each layer, the test was repeated at least three times on separate locations to ensure its repeatability.

Results and Discussion

Morphology of Carboxylated Diblock/Triblock Blended Gels. The structure of a physically cross-linked D/T1 gel was investigated by small-angle X-ray scattering. These experiments have allowed us to investigate the kinetics and temperature dependence of the structural formation of various gels. Figure 3 shows the scattered intensity over a range of momentum transfer, from $q = 0.06$ to 0.5 nm^{-1}, for a gel with volume fraction, Φp, equal to 0.25. Data in Figure 3a were obtained as the polymer gel was heated at a rate of 2 °C/min, from room temperature to 81 °C. At lower temperatures, from 26 to 40 °C, there is a very strong intensity peak around a q value of 0.19 nm^{-1} and a smaller peak near $q = 0.31$ nm^{-1}. These two peaks correspond to the structure factor, whereas a broad intensity peak near $q = 0.65$ nm^{-1} signifies the position of the form factor (not shown in Figure 3). At intermediate temperatures, as the polymer gel approaches its gel point, there is a shift in the intensity peak to lower q values. In this temperature regime, the broadening of the maximum interference peak and shift of the form factor to lower q values indicates that the glassy PMMA domains are increasing in size. At the highest temperatures, from 65 to 80 °C, there is a pronounced decrease in the maximum intensity, indicating that the ordering of the domains within the solvent/PNBA matrix is lost, as the gel undergoes a phase transformation from an elastic solid to a viscous liquid.[20] Within this temperature regime, the maximum interference peak shifts back to lower values, approaching the room-temperature interference peak position.

The cooling cycle of the gel from elevated temperatures to room temperature exhibits similar behavior to the heating cycle of the sample, as seen in Figure 3b. Upon cooling, we do not observe a pronounced peak in the scattering data at elevated temperatures (80 °C) whereas we notice a strong intensity peak close to 1.8 nm^{-1} for the room-temperature scan. Again, we see the shift in q_{max}, the q value corresponding to the maximum intensity, from higher q's in the high-temperature regime, to lower q's in the intermediate temperature regime to higher q's again at low temperatures.

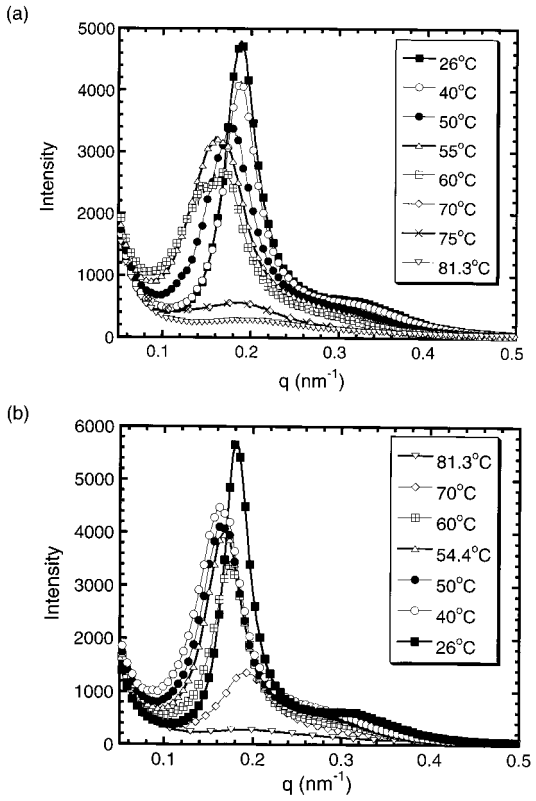

Figure 3. Small-angle X-ray scattering patterns from a carboxylated D/T1 gel with $\Phi_p = 0.25$ over a temperature range from $T = 26$ to 81 °C. Parts a and b show the patterns from the heating and cooling cycles, respectively, for gels ramped at 2 °C/min.

For the gels based upon the carboxylated diblock/triblock (D/T1) copolymer, we have investigated the effect of polymer concentration on the gel's structural formation. Figure 4 compares typical room-temperature scattering patterns for 5, 15, and 25 vol % polymer gels. As the polymer concentration within the gel increases, we observe an increase in I_{max}, the maximum intensity of the scattering pattern, and a shift in the peak to greater q's, indicating that the spacing between the PMMA domains is decreasing. The second local maximum in the curve, near $q = 0.3$ nm^{-1}, exhibits a stronger peak at higher polymer concentrations. In addition, the form factor becomes noticeable at higher concentrations, where we observe a local peak in the scattering pattern at $q = 0.65$ nm^{-1} for $\Phi_p = 0.25$. This broad peak of the form factor at higher q values suggests a gel structure with domain radii of approximately 9 nm, based upon the calculation of the position of a sphere's form factor.[3] So, as we dilute out the three-dimensional network with more solvent molecules, the distances between the glassy PMMA domains increase, and the size of these domains decreases. This observation is consistent with work performed by Mischenko et al., who showed that for polystyrene-*block*-rubber-*block*-polystyrene gels, as the polymer concentration increases, the PS domains increase in size and become more closely packed.[3]

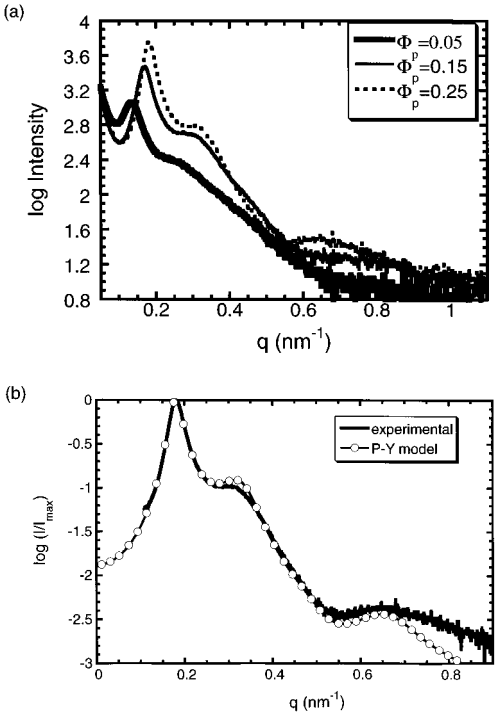

Figure 4. (a) Concentration dependence of the small-angle X-ray scattering patterns of carboxylated D/T1 gels with $\Phi_p = 0.05$, 0.15, and 0.25 at $T = 26$ °C. (b) Experimental scattering pattern for carboxylated D/T1 gel with $\Phi_p = 0.25$ fitted with the hard-sphere Percus−Yevick model, with $r_o = 8.2$ nm, $R_{HS} = 19$ nm, and $\eta = 0.47$.

Using the Percus−Yevick disordered hard-sphere model,[25] we have fit the experimental scattering pattern for $\Phi_p = 0.25$. The comparison between the model and the experimental data is shown in Figure 4b. The intensities of the experimental and model curves are normalized by I_{max}. This hard-sphere model assumes a dense core of the PMMA domains, with radius r_o, surrounded by an outer shell of dissolved PNBA chains defining an effective hard-core radius, R_{HS}. Following the work of Mischenko et al.,[3] Kinning and Thomas,[26] and others,[1,2] we have modeled the microstructure of the gel as a liquid with interacting hard spheres, with volume fraction η. Using this method, the intensity of the scattering pattern may be expressed as the product of a constant, K, the number of scattering units, N, the form factor, $P(q)$, and the structure factor, $S(q)$, as shown in eq 1.

$$I(q) = KNP(q)\,S(q) \tag{1}$$

The structure factor accounts for the interactions between the hard spheres or PMMA domains, whereas the form factor provides insight as to the size of these PMMA aggregates, which contribute to the scattering pattern at q values near 0.65 nm^{-1}. We have fit the experimental scattering data using an averaged expression for $P(q)$ with a diffuse boundary area.[3] As shown in Figure 4b, we obtain fairly good agreement between the experimental data and hard-sphere modeling curve, in which the first two peaks in intensity correspond to the structure factor and the broad peak at higher q values is fit with the form factor. For this scattering pattern, we have used $r_o = 8.2$ nm, $R_{HS} = 19$ nm, and $\eta = 0.47$.

To examine the differences between the heating and cooling cycles of the 25 vol % D/T gels more closely, we

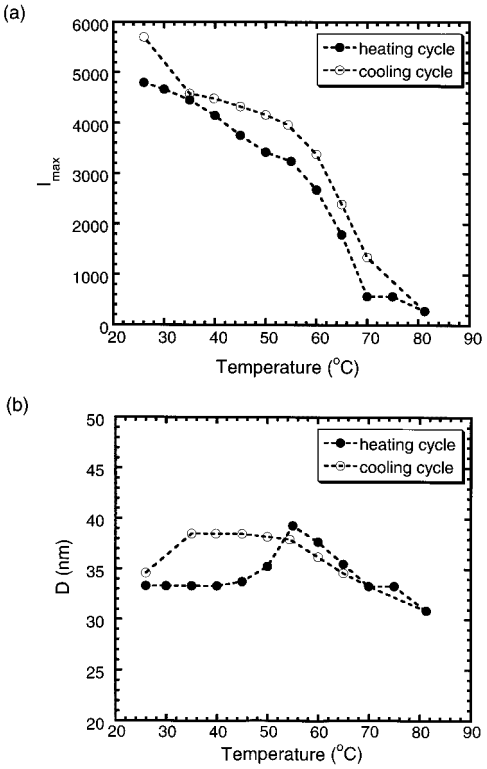

Figure 5. (a) Temperature dependence of the maximum scattered intensity for carboxylated D/T1 gel with $\Phi_p = 0.25$, during a heating/cooling cycle from $T = 25$ to 81 °C, with 2 °C/min heating/cooling rate. (b) Effect of temperature on interdomain spacing, D, for carboxylated D/T1 gel with $\Phi_p = 0.25$, subjected to a heating/cooling cycle with 2 °C/min ramp.

compare I_{max} and the approximate interdomain spacing, D (defined operationally as $D = 2\pi/q_{max}$), over a temperature range from 26 to 81 °C. Figure 5 illustrates the equilibrium structural development that occurs in the carboxylated D/T gel as the gel is heated above its gel point and cooled to room temperature. In Figure 5a, we show that the heating/cooling cycle is fairly reversible, but the intensity of the maximum interference peak is slightly lower for scans taken during the heating ramp than those obtained during the cooling cycle. For this temperature range, we compare the interdomain spacing of PMMA aggregates in Figure 5b. As we heat the gel from room temperature to 50 °C, the domain spacing of approximately 33.5 nm remains constant. This behavior is similar to previous rheological studies on the gel, which indicate that the dynamic moduli do not change until the gel point, ∼60−65 °C, is approached.[20] Close to the gel point, the interdomain spacing increases sharply and begins to decrease again as the gel completes its transition to a viscous liquid state. As the polymer gel is cooled from 80 °C to its gel transition temperature, the heating/cooling cycle is very reversible, as indicated by the nearly overlaying points of D as a function of temperature. Below the gel point, the interdomain spacings are larger on cooling than on heating. However, after a period of a few minutes at room temperature, the gel's structure returns to its original state. At elevated temperatures, scattering is characteristic of a disordered structure, as confirmed by our rheological studies. For a D/T gel with Φ_p equal to 0.05, the scattering pattern of the sample after being cooled to room temperature from above its gel point was identical to a pattern taken 433 min later at the same

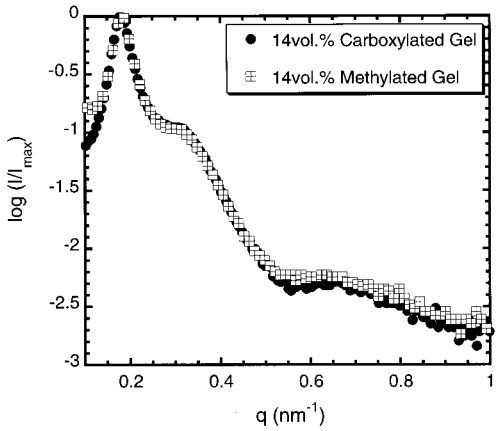

Figure 6. Comparison of normalized SAXS patterns for carboxylated and methylated T1 gels with $\Phi_p = 0.14$ at $T =$ 25 °C.

temperature. This result further confirms the equilibrium nature of the gel state.

Previous studies on these polyacrylate gels indicate that they are an excellent model system for probing weak adhesive interactions between two surfaces in contact.[22] Within the rubbery PNBA midblock, a few mole percent of acrylic acid groups forms during the conversion of the parent PMMA−poly(*tert*-butyl acrylate)−PMMA triblock to PMMA−PNBA−PMMA. These acrylic acid moieties do not affect the adhesive behavior of the swollen polymer gel.[22] Here, we are interested in understanding to what extent these functional groups contribute to the development of the gel's microstructure and how they affect the adhesive behavior of "dried" polymers processed through a gel casting method. Axisymmetric adhesion tests performed on a carboxylated homopolymer show that the adhesive strength of these polymers is enhanced as compared to a methylated version of the same homopolymer. Specifically, acrylic acid moieties have been shown to have an effect on the adhesive behavior of a cross-linked PNBA elastomer in contact with a variety of glassy polymers.[15] In the following section, we explore the effects of these reactive groups on the structural development in the triblock copolymer gels. In a subsequent section, these findings are compared to results from adhesion tests of dried gels.

Effect of Acrylic Acid Moieties on the Morphology of Triblock Gels. We have compared the carboxylated (C-T1) and methylated (M-T1) ABA type triblock copolymer gels, using small-angle X-ray scattering experiments, to examine the role acrylic acid groups play in the formation of the gel's structure. At room temperature, the structures of the carboxylated and methylated gels are identical, suggesting that the very low fraction of acrylic acid functional groups in the gel do not contribute to its structural development. In Figure 6, we compare the intensity versus q values of a carboxylated T1 gel and methylated T1 gel at 25 °C, with Φ_p equal to 0.14. The position and intensity of the maximum interference peak indicate that the spacings between PMMA domains are unaffected by the addition of a few mole percent of acrylic acid groups in the carboxylated gel. In addition, the overlaying points of the scattering patterns at higher q values (form factor) suggest that the sizes of the PMMA aggregates are identical for both samples. These observations are consistent with our previous work where there were no

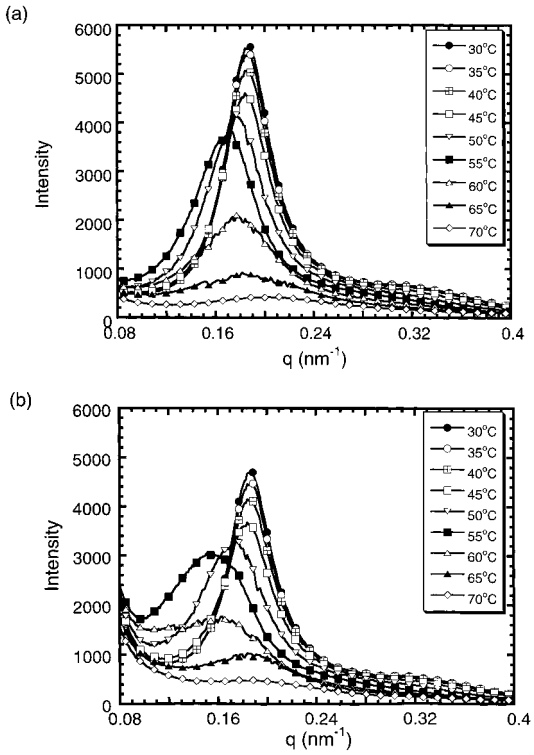

Figure 7. SAXS patterns of (a) carboxylated T1 gel and (b) methylated T1 gel with $\Phi_p = 0.14$. Samples were heated from $T = 30$ to 70 °C at a rate of 2 °C/min.

obvious differences between the mechanical properties of the two triblock copolymer gels at room temperature.[22]

While the room-temperature scattering patterns of the carboxylated and methylated T1 gels appear to be the same, we notice several differences between these gels at elevated temperatures. Figure 7 compares samples of T1 with Φ_p equal to 0.14, for a heating cycle in the temperature range from 30 to 70 °C. Both the carboxylated (Figure 7a) and methylated (Figure 7b) gels exhibit a pronounced intensity peak near $q = 0.188$ nm^{-1}, corresponding to an interdomain spacing close to 33.6 nm, at a temperature of 30 °C. In fact, very few differences between the two gels are observed until the samples are heated to 55 °C, close to the gel point. Previous rheological experiments have indicated that the mechanical properties such as the storage and loss moduli only begin to change as the swollen polymer is heated to temperatures approaching its solid/liquid transition. At temperatures of 55 °C and higher, we notice an interesting difference between the two samples; the T1 methylated gel's interference peak broadens and shifts to lower q's, whereas the T1 carboxylated gel's interference peak remains sharp and shows only a slight shift toward lower q's. For both samples, between 65 and 70 °C, the intensity peak shifts back toward its position at lower temperatures. At intermediate temperatures, as the polymer/solvent interactions become more favorable for the PMMA, we observe a loss of the short-range ordering of the glassy block aggregates. In this temperature regime, the polymer chains are more mobile within the solvent matrix, and the complexation of acrylic acid moieties within the rubbery midblock is able to influence the network's local structure. Similar effects have been observed in bulk ionomers.[27,28]

Figures 6 and 7 highlight the idea that a few mole percent of acrylic acid groups within the rubbery mid-

block PNBA will alter neither the interdomain distances nor the domain sizes of the PMMA. Although the microstructure for the carboxylated (C-T1) and methylated (M-T1) triblock copolymer gels appears to be the same at room temperature, acrylic acid moieties do influence the local structure of the gel network at elevated temperatures, close to the gel point. This agreement in structure at room temperature suggests that it is possible to tailor the properties of a polyacrylate polymer, by either adding or removing reactive groups such as acrylic acid moieties, while still maintaining a particular microstructure within the gel. As we will discuss later in the paper, by removing solvent from the swollen polymer, a "dried" polymer adhesive can be processed in which the microstructure has been controlled through a gel casting technique. The size and spacing of PMMA domains can be altered, by diluting out the polymer entanglements with varying amount of solvent molecules. More importantly, the volume fraction of polymer within the gel will influence the fraction of bridging molecules between PMMA domains. The fraction of these bridging chains will directly affect the elastic and mechanical properties of the swollen and "dried" polymers.

Aside from chemically converting functional groups within the triblock copolymer, blending the copolymer with a homopolymer is another viable route for altering the properties of the gel. We explore the effects of stereocomplexation of the syndiotactic PMMA end blocks with a low molecular weight isotactic PMMA homopolymer. By strengthening these anchoring domains within the gel's structure, it is possible to increase the stability of the gel to higher temperatures, as shown by Yu and Jerome.[14] In the next section, we discuss effects of the homopolymer isotactic PMMA on the gel's structural development.

Effect of Stereocomplexation on Carboxylated Diblock/Triblock Blended Gels. The addition of an isotactic PMMA homopolymer to the carboxylated D/T1 gel has a large impact on the gel's structural, kinetic, and mechanical behavior. These effects are remarkable considering the fact that the gel is comprised mostly of solvent (90 wt %) with only about 10 wt % polymer, of which the syndiotactic PMMA accounts for approximately 3% of this total. The isotactic PMMA homopolymer is only added in a 1:2 weight ratio to the sPMMA blocks, yet, its role in the development of the gel is significant. For this reason, we continue to refer to Φ_p as the fraction of copolymer in the gel, excluding the addition of the isotactic homopolymer. We have investigated the effects of the stereocomplexation of the D/T1 gels by performing small-angle X-ray scattering experiments on samples with $\Phi_p = 0.05$ and 0.15. At room temperature, we observe the same trend as the D/T1 gels without the iPMMA; as the polymer concentration within the gel increases, the distance between PMMA domains decreases and the recorded intensity increases. However, the response of the iPMMA gels during heating and cooling cycles differs from the D/T1 gels with no added iPMMA. In Figure 8, we show the scattering patterns of a 5 vol % polymer gel heated from 25 to 100 °C (Figure 8a) and cooled from elevated temperatures to 26 °C (Figure 8b.) If we compare Figure 8a to Figure 3a, we notice three distinct differences between the response of the iPMMA D/T1 gel and the regular D/T1 gel. As the iPMMA gel is heated, the position of the maximum intensity peak remains constant from room temperature to elevated temperatures, but its magnitude decreases with increasing temperature. In contrast, the regular D/T gels exhibit changes in interdomain spacing throughout the heating and cooling cycles. In addition, the stabilization of the PMMA aggregates in the iPMMA gels is apparent at elevated temperatures. There appears to be some degree of ordered structure up to temperatures exceeding 70 °C for these materials, whereas in the regular D/T1 gels, this local ordering is lost for temperatures greater than 60 °C. Last, comparisons of Figures 3 and 8 reveal that the distance between PMMA domains is larger for the iPMMA gel samples than the regular gels. Also, the interference peak of the form factor is more defined for the regular D/T gels than for those blended with the isotactic PMMA homopolymer.

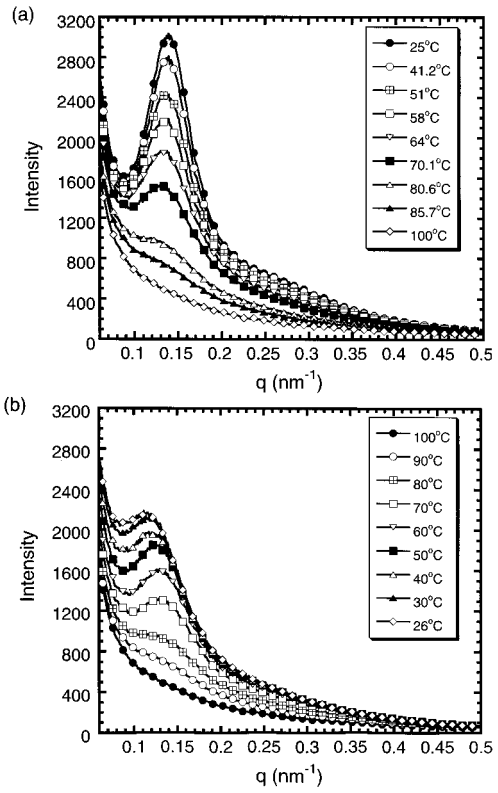

Figure 8. Scattering patterns showing effects of isotactic PMMA homopolymer blended with the carboxylated triblock copolymer gel, D/T1. Part a displays SAXS patterns for gel with $\Phi_p = 0.05$ heated from $T = 25$ to 100 °C at a rate of 2 °C/min, and part b reveals structural formation of gel upon cooling from $T = 100$ °C to room temperature, at 2 °C/min.

Kinetics and Rheological/Structure Relationships for D/T and D/T iPMMA Gels. While we have commented on the gel's structural development within different temperature regimes, we have not yet discussed the kinetics of network formation. For a carboxylated iPMMA gel we have monitored the development of the gel's microstructure through a heating/cooling cycle and steady-state holding period. In Figure 9, we show the evolution of the scattering pattern for this iPMMA D/T gel with Φ_p equal to 0.05 and the respective temperature−time profile of the sample. At point A, we obtain a scattering pattern for the sample at room temperature, followed by a heating ramp of 2 °C/min until the sample reaches point B, at a temperature of 100 °C. At this point, there are no distinctive peaks above the baseline within the scattering pattern. The sample is then cooled to 25 °C and held at low

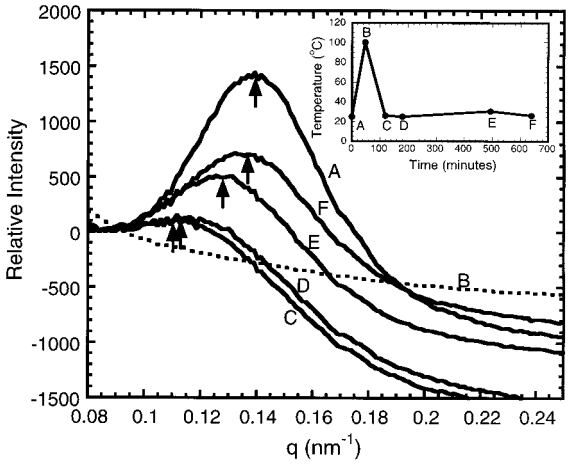

Figure 9. Evolution of small-angle X-ray scattering pattern of carboxylated D/T1 gel with $\Phi_p = 0.05$, blended with isotactic PMMA homopolymer. Scans were obtained at points indicated on the temperature profile (inset). Dotted line represents scattering pattern of point B, where a distinct interference peak and constant baseline value are not observed. Location of q_{max} is indicated by the arrow. Profiles were shifted vertically as described in the text.

temperatures for over 500 min in order to evaluate any time-dependent structural changes within the sample.

In Figure 9, we plot the relative intensity, obtained by shifting the data vertically so that for a given curve the minimum intensity occurs at zero along the *y*-axis, versus the momentum transfer, *q*. This normalization technique provides a clear picture of the effect of temperature on I_{max}. The scattering pattern at 100 °C (point B) is normalized by shifting the intensity curve vertically so that is crosses with the other curves at $q = 0.09$ nm^{-1}, since the intensity of this pattern decreases continuously over the full *q* range. At room temperature (point A), the relative intensity of the maximum interference peak is strong and occurs at $q_{max} = 0.14$ nm^{-1}. However, after the sample is heated to 100 °C (point B) and cooled to room temperature (point C), the relative intensity of the curve's maximum above the baseline has been dramatically reduced. Also, we observe a decrease in q_{max}. The scattering patterns at points C, D, E, and F show that the gel exhibits a time-dependent response in its morphological development. In fact, between points C and D, the gel is held at constant temperature for 60 min, and only a slight change in interdomain spacing is observed. Over a period of 500 min, we do observe the fact that the PMMA aggregates pack more closely within the solvent/rubbery matrix as indicated by the increase in q_{max}. Also, the interference peak's relative intensity increases over time as the sample is held at room temperature. The iPMMA gel with 15 vol % D/T1 polymer shows similar behavior, in that the *d* spacing increases after a heating/cooling cycle yet regains its original spacing after a hold time at room temperature.

Clearly, temperature greatly impacts the three-dimensional network within both the iPMMA D/T1 and regular D/T1 gels. We have commented on several of the differences between these polymer samples earlier, and we believe it is worthwhile to further illustrate the significance of the stereocomplexation of the end blocks within the triblock copolymer by making a direct comparison between the gel samples. In Figure 10, we compare a carboxylated D/T1 gel with $\Phi_p = 0.05$, for the "regular" gel sample and the "iPMMA" gel sample.

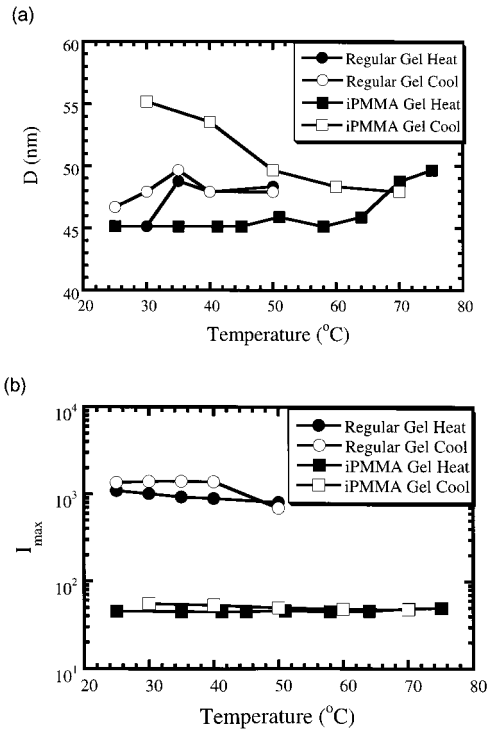

Figure 10. Interdomain spacings (part a) and intensity of maximum interference peak (part b) for a regular gel and iPMMA modified gel with $\Phi_p = 0.05$ are shown. "Regular" gels were formed by diluting the D/T1 copolymer with a selective solvent for the midblock, and "iPMMA gels" were formed by blending the isotactic homopolymer PMMA with the regular gel. Filled symbols indicate temperatures during heating cycles whereas open symbols indicate patterns taken during cooling cycles.

Both samples have been heated to temperatures above their individual gel points, so that the gels are able to flow as viscous liquids. We plot the interdomain spacings, *D*, and maximum intensities of the interference peaks as a function of temperature in Figure 10. In Figure 10a, we illustrate that the structural formation of both gels is highly time dependent. In addition, Figure 10 shows that the stereocomplexation of the iPMMA stabilizes the gels at elevated temperatures, as compared to the regular gels, which show no discernible interference peak above 60 °C. While the interdomain spacings do not exhibit a reversible equilibrium process (Figure 10a), the maximum intensities of the interference peaks (Figure 10b), in both the iPMMA gels and regular gels, seem to deviate only slightly between the heating and cooling cycles.

The SAXS patterns of the iPMMA gels show that they retain structural order to higher temperatures than do the D/T1 gels that do not contain iPMMA. Addition of iPMMA also increases the time it takes for the structure of the gel to equilibrate. While the morphological development within the iPMMA gels differs from that in the regular gels, it is important to understand how this isotactic homopolymer can also effect its mechanical properties. We have already characterized the regular gel using dynamic oscillatory shear experiments, described previously.[20] Here, we compare these findings to the behavior of the D/T1 gels blended with the low molecular weight isotactic homopolymer. In Figure 11a, we show the response of the storage and loss moduli of a 5 vol % iPMMA D/T gel over a range of frequencies. As seen in the "regular" gels, G' is orders of magnitude greater than G'' and is unaffected by the change in

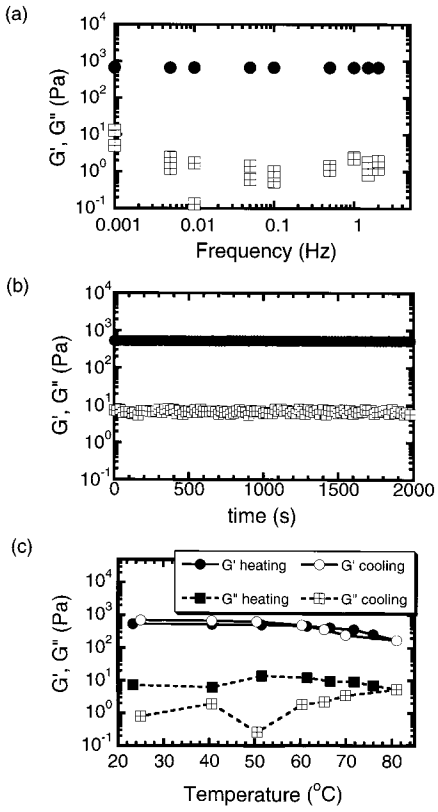

Figure 11. Dynamic shear moduli of carboxylated D/T1 gel with $\Phi_p = 0.05$ blended with isotactic PMMA homopolymer. (a) Frequency dependence of storage (G') and loss (G'') moduli of gel over range 1×10^{-3} to 2 Hz at $T = 25$ °C. (b) Oscillatory experiment using 1 Hz frequency shows time dependence of gel at $T = 25$ °C over a time period of 2000 s, after sample is cooled from $T = 80$ °C. (c) Effect of temperature on G' and G'' during heating and cooling cycle from $T = 25$ to 80 °C, as gel is oscillated with 1 Hz frequency. Filled symbols indicate data acquired during heating cycle.

frequency from 1×10^{-3} to 2 Hz. The scatter in the loss moduli is attributed to the fact that the rheometer is not sensitive to these low values. Using a frequency of 1 Hz, we observe that, for a gel heated to 80 °C and immediately cooled to room temperature, the modulus does not change over a time period of 2000 s, as seen in Figure 11b. At room temperature, the gel behaves as an elastic solid with $G' \gg G''$. Again, this behavior is identical to the response of the "regular" gel as it is cooled from elevated temperatures to room temperature and oscillated for an extended period of time.

Even though the iPMMA gels and regular gels behave as elastic solids and show no frequency dependence at room temperature, as these samples are heated, differences in the temperature corresponding to the gel point are noticeable. For the regular gel, G'' begins to exceed G' near 60 °C, whereas for the iPMMA gel, even at a temperature of 80 °C, G' is much larger than G''. Figure 11c illustrates the response of the storage and loss moduli during a heating and cooling cycle for an iPMMA gel with Φ_p equal to 0.05. Although the temperature corresponding to a gel point of the iPMMA exceeds the range of our experimental apparatus, the solid/liquid transition temperature is estimated to be around 90−95 °C, based upon observations of the flow of the gel. The addition of the isotactic homopolymer strengthens the network structure in that it remains stable at higher temperatures.[14]

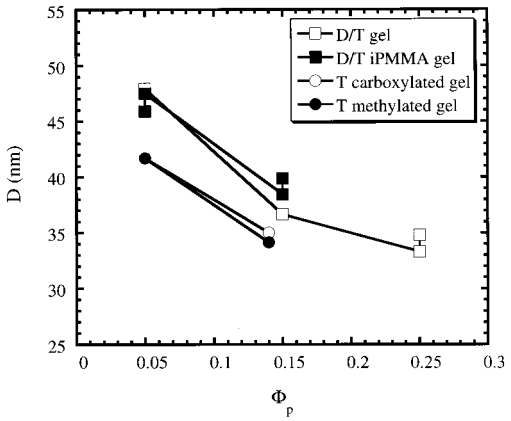

Figure 12. Effect of polymer volume fraction in the gel on interdomain spacings. We compare the D/T regular gels, D/T iPMMA gels, T carboxylated gels, and T methylated gels.

To summarize our results from the variety of diblock/triblock copolymer gels studied using the SAXS experiments, we have plotted the interdomain spacing, D, as a function of the volume fraction polymer in the gels. Figure 12 includes data for the diblock/triblock (D/T1) gels with and without the addition of the iPMMA homopolymer and for the carboxylated (C-T1) and methylated (M-T1) triblock copolymer gels. As the graph illustrates, as the polymer concentration increases in the gel, the distance between the aggregates decreases. Also, the presence of acrylic acid moieties within the gel does not seem to have much of an effect on the gel's microstructure.

While the SAXS interference patterns and corresponding interdomain spacings have focused on the swollen gels up to this point, in many situations it is convenient to remove the solvent from these materials to recover the triblock copolymer. In our work, we investigated the effect of processing these ABA triblock copolymers by forming either a swollen gel or solution as an intermediate step. We have studied both the adhesive and structural properties of "dried" polymer layers formed in this manner. These results are presented in the following sections.

Processing of Triblock Copolymers via Gels and Solutions. In situ SAXS experiments were performed to investigate the effect of solvent removal on the structure of swollen triblock copolymer gels. In Figure 13a, we show the interference patterns for a D/T1 gel with $\Phi_p = 0.15$ in butanol that was dried for 105 min at a temperature below its gel point. As solvent is evaporated from the sample, I_{max} decreases, but the spacing of PMMA domains essentially remains the same. The noticeable decrease in I_{max} is attributed to the decrease in electron density differences between the PMMA domains and surrounding matrix. Because of the geometry of our sample, we are essentially probing the effects of a one-dimensional drying process of a constrained, thin film. While the domains become closer in the film thickness direction, the domains remain evenly spaced in the lateral direction, as shown with these experiments. Also during this drying process, the form factor becomes indistinguishable from the baseline as electron density differences between the PMMA and surrounding matrix decrease. On the basis of these observations, we believe that although a large amount of solvent is removed from the swollen gel (approximately 85 vol %), the spacings of PMMA aggregates do not change. It is possible that the size of these domains

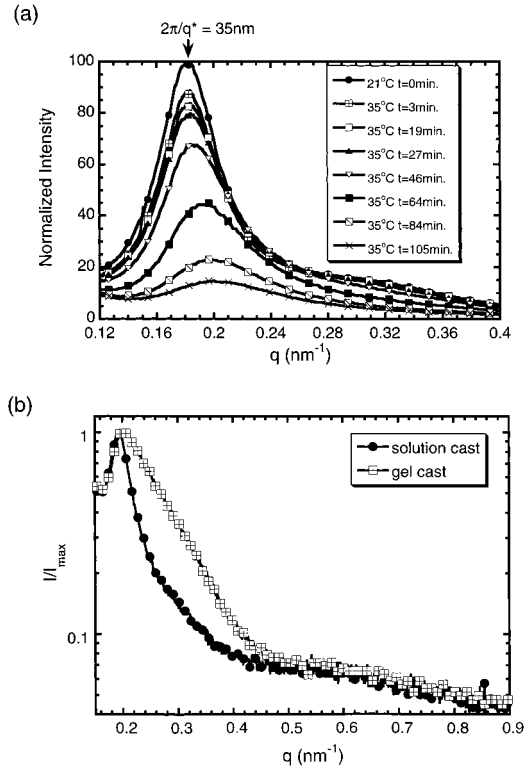

Figure 13. (a) SAXS interference patterns of in situ drying of polymer gel below its gel point with $\Phi_p = 0.15$ in butanol. The top curve indicates a room-temperature scan followed by sequential patterns for various times at 35 °C. (b) Comparison of SAXS patterns for a dried solution cast and dried gel cast D/T1 layer with $\Phi_p = 0.25$.

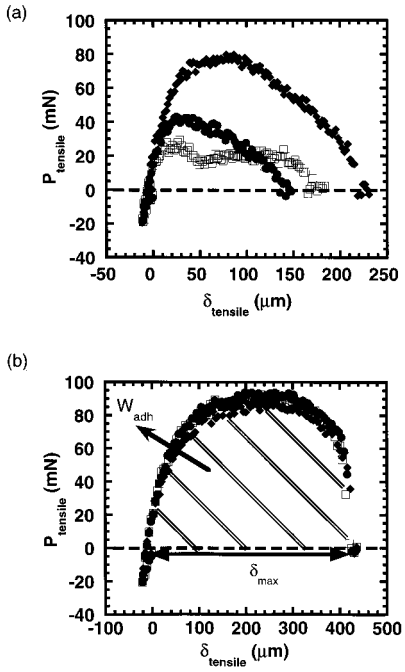

Figure 14. Comparison of load−displacement relationships from adhesion tests performed on dried carboxylated D/T1 copolymers processed via solution casting, part a, and gel casting, part b, techniques. Symbols indicate separate adhesion experiments conducted on the same polymer layer. In part b, the maximum tensile displacement, δ_{max}, is illustrated.

may be increasing during this drying process, but this phenomenon is inconclusive due to our inability to resolve the scattering patterns in the form factor's q range for dried gels.

We have processed triblock copolymer layers by forming both swollen gels and solutions, casting films, and then evaporating off the solvent from the layers. The swollen gels were formed by diluting the triblock copolymer in a selective solvent for the midblock, whereas the solutions were formed by dissolving the polymer in a solvent that is nonpreferential for either the A or B blocks. Figure 13b illustrates the normalized scattering patterns for solution cast and gel cast layers processed with $\Phi_p = 0.25$. While the width of the maximum interference peak is much larger for the gel cast sample, the position of this peak is very similar for both the solution and gel cast layers.

The formation of bridging chains between these aggregates may be the most significant structural factor affecting the mechanical properties of the gels, even under conditions where identical scattering patterns are obtained. By diluting the triblock copolymer in a selective solvent for the PNBA, the PMMA chains aggregate into domains within the solvent/PNBA matrix at room temperature. This gel network forms equilibrium structures with bridging fractions that are presumably quite reproducible. In contrast, when the copolymer is dissolved in a solvent that is not selective for either block, the structural formation is a nonequilibrium process, yielding a dried "solvent cast" polymer with an irreproducible structure. In the following section, we demonstrate that it is possible to utilize the gelation mechanisms to create "dried" polymer films with reproducible adhesive properties. We discuss our testing methodology for quantifying the adhesive response of these layers and compare the adhesive behavior of "dried" carboxylated and methylated T1 adhesive films. Last, we investigate the effects of polymer concentration in the swollen state to the "dried" polymer layer's final adhesive properties.

Effect of Gel Casting Processing Technique on Adhesive Properties. We quantify the adhesive behavior of "dried" polymer layers by performing axisymmetric adhesion tests in which a glass, hemispherical indenter is pressed into an adhesive layer, with a thickness ranging from 38 to 280 μm. Simultaneous measurements of the applied load, displacement between the surfaces, and circular contact area are recorded as the two bodies are pressed together with a maximum loading force of 25 mN and then separated. Figure 2 shows this experimental geometry. The crosshead velocities used for the D/T1 and T1 polymer layers were 2.5 and 2 μm/s, respectively. Tack curves that describe the load−displacement relationship for each test are used to compare the adhesive behavior of different polymer layers. Similar tests have been used previously for quantifying the adhesive properties of pressure-sensitive adhesives.[29−31] In this work, we define a positive force, $P_{tensile}$, as a tensile load and the zero displacement point as the position where the indenter establishes contact with the layer.

In Figure 14, we compare tack curves for two different 250 μm thick D/T1 copolymer layers that have been processed using either the solution casting or gel casting techniques. For the polymers processed with the solution casting method, the data are very irreproducible, as shown in Figure 14a. Both the maximum pull-off force and the displacement at which the load returns to zero vary for each of the three tests. In contrast, Figure 14b shows that, for the layers processed by solvent evaporation from a swollen gel with Φ_p equal

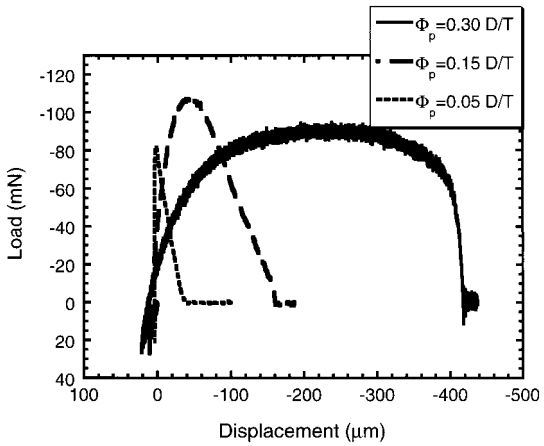

Figure 15. Adhesive behavior of dried carboxylated D/T copolymer samples formed from gels with $\Phi_p = 0.05$, 0.15, and 0.30. Thicknesses of the dried layers were 38 μm ($\Phi_p = 0.05$), 257 μm ($\Phi_p = 0.15$), and 254 μm ($\Phi_p = 0.30$.)

to 0.30, the data points for all three tests overlay remarkably. Layers produced from gels rather than solutions showed superior strength, as indicated by the higher pull-off force and greater extension for separation from the indenter. This comparison effectively demonstrates how the processing techniques of forming a polymer influence both microstructures and, in turn, the adhesive properties of a material. As discussed in the previous section, we believe that the fraction of bridging molecules is the dominating mechanism for influencing the properties of the dried copolymer layers. Figure 13 illustrated the idea that by forming a swollen gel the structure essentially remained intact even though solvent was removed from its network. Although both the solution and gel cast dried films exhibited similar PMMA domain spacings, we assert here that it is the bridging of PNBA chains between these aggregates that form in the swollen state and affect the adhesive and mechanical properties of the dried material.

To quantify the amount of energy required to separate the adhesive from the probe, we integrate the area under the tack curve and normalize this energy by the maximum contact area, A_{max}, to obtain the overall work of adhesion, W_{adh}, as shown in eq 2. The shaded area in Figure 14b corresponds to the integral presented in the following equation.

$$W_{adh} = \frac{\int P \, d\delta}{A_{max}} \tag{2}$$

Measurements of W_{adh} provide a convenient method for comparing the adhesive energy of different polymer layers.[32−34] Figure 14b also illustrates the definition of δ_{max}, corresponding to the full range of displacement between the indenter and polymer layer during the unloading portion of the adhesion test.

Using this approach, we have compared the adhesive response of three "dried" D/T1 polymer layers formed from gels with polymer volume fractions of 0.05, 0.15, and 0.30. In Figure 15, we compare the tack curves obtained from each layer. Admittedly, this is not a very direct comparison, because the thickness of the 5 vol % sample is only 38 μm, whereas the thickness of the 15 and 30% samples range between 257 and 270 μm. While these thickness variations most certainly play a role in the quantifiable energies, we present this figure as an

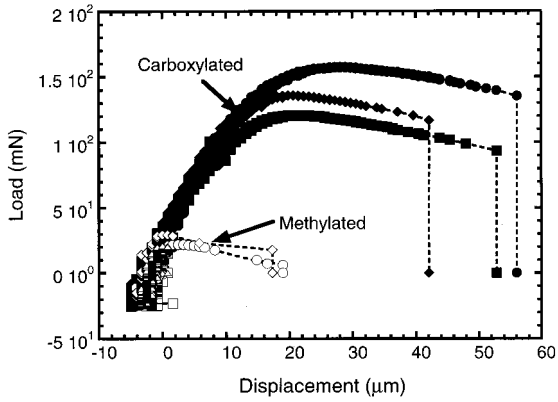

Figure 16. Comparison of adhesive response of dried carboxylated and methylated T1 copolymers formed from gels with $\Phi_p = 0.05$. The thickness of the dried layers was 76 μm.

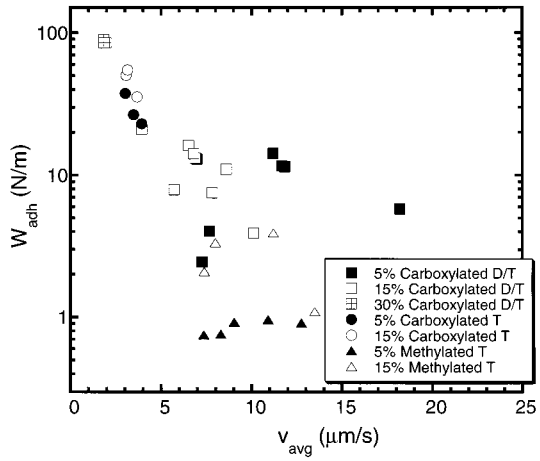

Figure 17. Effective work of adhesion versus the average crack tip velocity for dried layers. Data are included for carboxylated D/T blends formed from gels with $\Phi_p = 0.05$, 0.15, and 0.30, as are data from carboxylated and methylated triblock copolymers with $\Phi_p = 0.05$ and 0.15.

illustration of the wide variances between "dried" samples obtained from gels with different concentrations. For samples obtained from gels with $\Phi_p = 0.15$ and $\Phi_p = 0.30$, we notice large differences in δ_{max} and W_{adh}, even though the dried gels have similar thickness.

We apply this methodology in quantifying the adhesive behavior of polymer layers to our investigation of the effect of acrylic acid moieties within polyacrylates. Figure 16 depicts typical load−displacement relationships for methylated and carboxylated T1 layers with Φ_p equal to 0.05 and thickness of 76 μm. The differences between the methylated and carboxylated samples are significant; the acrylic acid functional groups within the carboxylated T1 polymer greatly enhance its adhesion with the glass indenter. If we compare the maximum pull-off load and displacement during the unloading part of the test, we see that the methylated samples are much weaker than the carboxylated samples. The carboxylated layers extend an additional 25−40 μm beyond the methylated samples on unloading and reach a 130 mN pull-off load, as compared to P_{max} near 30 mN for the methylated layers.

We can highlight the effect of the acrylic acid groups in the triblock copolymer by using the comparison shown in Figure 17, in which we plotted the effective work of adhesion, W_{adh}, versus v_{avg}, the average crack tip velocity for separating the glass probe from the gel

layer. These results may be compared to the peel test where W_{adh} essentially corresponds to the peel energy while v_{avg} relates to the velocity of the peeling test. Adhesives with slower average crack velocities dissipate more energy during the unloading portion of the test than polymers that separate quickly from the indenter at low loads and small displacements. We use this method to show that the carboxylated "dried" gels exhibit superior adhesion to the methylated "dried" gels. For each material test, we obtain one point along the W_{adh} versus v_{avg} curve. This value of W_{adh} is an averaged energy release rate during the test. The particular point corresponding to an individual test is determined by the adhesive strength of the material, its mechanical response, the experimental geometry, and the cross-head velocity. At this time, it is difficult to separate out differences between the 5 and 15 vol % samples, although the general trend indicates that higher polymer volume fractions will enhance the adhesive properties of the material. For dried layers formed from gels with $\Phi_p = 0.15$, the carboxylated triblock copolymers (C-T1) have an average W_{adh} of 46.8 N/m at $v_{avg} = 3.3$ μm/s, whereas the methylated triblock copolymers (M-T1) have an average effective work of adhesion close to 2.6 N/m at $v_{avg} = 10.0$ μm/s. Figure 17 also compares the effective work of adhesion for dried diblock/triblock (D/T1) blends formed from gels with $\Phi_p = 0.05$, 0.15, and 0.30. As shown in the SAXS experiments, as the polymer concentration increases within the gel, the PMMA domain sizes increase and pack more closely within the solvent/PNBA matrix. This arrangement promotes polymer bridging between the domains thus affecting the elastic properties of the polymer.

The adhesion tests described in this paper confirm the idea that the polymer's processing method will affect the adhesive properties of the polymer sample. Coupled with the small-angle X-ray scattering results, these experiments show that forming a "dried" polymer via a gel casting technique allows one to control the microstructure of the final product by varying the amount of solvent in the gel. Since interdomain distances, intradomain sizes, and polymer bridges are dependent on the relative amount of solvent within the gel, one can tailor the network formation of the gel to form polymers with varying adhesive and mechanical properties. In our work, we have demonstrated that chemical conversions of acidic side chains to methylated groups within the triblock copolymer will decrease the adhesive nature of the "dried" polymer, while still maintaining its overall structural morphology.

Summary

We have used small-angle X-ray scattering experiments to examine the microstructure of ABA triblock copolymer gels, formed by diluting the polymer with a selective solvent for the B block. By creating gels with a range of volume fractions of polymer from 0.05 to 0.30, we have investigated the effects of both concentration and temperature on the development of the gel's structure. At room temperature, the PMMA end blocks aggregate into spherical domains within the PNBA/solvent matrix. We evaluate different polymers formed from this method by probing the adhesive behavior of "dried" polymer layers produced via a swollen gel state. Our main conclusions are as follows:

1. The composition and temperature of the gel govern the development of its final microstructure, by affecting the size of the PMMA domains and the spacings between these domains. With increasing polymer concentrations within the gel, the spherical PMMA domains pack more closely and increase in size. At temperatures close to the gel point, the broadening of the maximum interference peak and decrease in I_{max} suggest that the physically bound network is beginning to disorder.

2. A few mole percent of acrylic acid moieties within the rubbery PNBA chains does not affect the structural formation of the gel, as shown by comparisons to a "methylated" version of an identical polymer. However, when the solvent is removed from the gel to create a "dried" polymer, these functional groups significantly affect the adhesive properties of the polymer layer, increasing the effective work of adhesion by a factor of 18.

3. Stereocomplexation of the syndiotactic end blocks of the triblock copolymer with a low molecular weight isotactic PMMA homopolymer provides an efficient method to strengthen the gel network. SAXS results indicate that addition of isotactic PMMA increases the thermal stability of the gel while increasing the time required for the equilibrium structure to develop at room temperature.

4. Dried polymer layers formed from the gel casting technique exhibit a reproducible structure and, hence, a reproducible mechanical response as probed by axisymmetric adhesion experiments. Gel casting is an excellent method for tailoring the properties of the polymer for a desired application because the microstructure can be readily controlled in the swollen state.

Acknowledgment. We gratefully acknowledge Prof. W. Burghardt, D. Cinader, V. Ugaz, F. Caputo, and J. Quintana for assistance with the SAXS experiments. Use of the Advanced Photon Source was supported by the U.S. Department of Energy, Basic Energy Sciences, Office of Energy Research, under Contract W-31-109-Eng-38. Project support from NSF Grant DMR-9457923 is also acknowledged.

References and Notes

(1) Mortensen, K.; Pedersen, J. S. *Macromolecules* **1993**, *26*, 805.
(2) Kleppinger, R.; Reynders, K.; Mischenko, N.; Overbergh, N.; Koch, M. H. J.; Mortensen, K.; Reynaers, H. *Macromolecules* **1997**, *30*, 7008.
(3) Mischenko, N.; Reynders, K.; Koch, M. H. J.; Mortensen, K.; Pedersen, J. S.; Fontaine, F.; Graulus, R.; Reynaers, H. *Macromolecules* **1995**, *28*, 2054.
(4) Mischenko, N.; Reynders, K.; Mortensen, K.; Scherrenberg, R.; Fontaine, F.; Graulus, R.; Reynaers, H. *Macromolecules* **1994**, *27*, 2345.
(5) Reynders, K.; Mischenko, N.; Kleppinger, R.; Reynaers, H.; Koch, M. H. J.; Mortensen, K. *J. Appl. Crystallogr.* **1997**, *30*, 684.
(6) Balsara, N. P.; Tirrell, M.; Lodge, T. P. *Macromolecules* **1991**, *24*, 1975.
(7) ten Brinke, G.; Hadziioannou, G. *Macromolecules* **1987**, *20*, 486.
(8) Yu, J. M.; Jerome, R.; Teyssie, P. *Polymer* **1997**, *38*, 347.
(9) Brown, W.; Schillen, K.; Almgren, M.; Hvidt, S.; Bahadur, P. *J. Phys. Chem.* **1991**, *95*, 1850.
(10) Laurer, J. H.; Mulling, J. F.; Khan, S. A.; Spontak, R. J.; Bukovnik, R. *J. Polym. Sci., Part B: Polym. Phys.* **1998**, *36*, 2379.
(11) Kleppinger, R.; van Es, M.; Mischenko, N.; Koch, M. H. J.; Reynaers, H. *Macromolecules* **1998**, *31*, 5805.
(12) Quintana, J. R.; Diaz, E.; Katime, I. *Macromol. Chem. Phys.* **1996**, *197*, 3017.
(13) Reynders, K.; Mischenko, N.; Mortensen, K.; Overbergh, N.; Reynaers, H. *Macromolecules* **1995**, *28*, 8699.
(14) Yu, J. M.; Jerome, R. *Macromolecules* **1996**, *29*, 8371.
(15) Ahn, D.; Shull, K. R. *Langmuir* **1998**, *14*, 3637.

(16) Kano, Y.; Ushiki, H.; Akiyama, S. *J. Adhes.* **1993**, *43*, 223.
(17) Chan, H.-K.; Howard, G. *J. Adhes.* **1978**, *9*, 279.
(18) Gong, L. Z.; Wool, R. P. *Bull. Am. Phys. Soc.* **1997**, *42*, 464.
(19) Ahn, D.; Shull, K. R. *Macromolecules* **1996**, *29*, 4381.
(20) Mowery, C. L.; Crosby, A. J.; Ahn, D.; Shull, K. R. *Langmuir* **1997**, *13*, 6101.
(21) Varshney, S. K.; Jacobs, C.; Hautekeer, J.-P.; Bayard, P.; Jérôme, R.; Fayt, R.; Teyssié, P. *Macromolecules* **1991**, *24*, 4997.
(22) Flanigan, C. M.; Shull, K. R. *Langmuir* **1999**, *15*, 4966.
(23) Aldrich Technical Information Bulletin, Number AL-180.
(24) Johnson, K. L.; Kendall, K.; Roberts, A. D. *Proc. R. Soc. London A* **1971**, *324*, 301.
(25) Percus, J. K.; Yevick, G. J. *J. Phys. Rev.* **1958**, *110*, 1.
(26) Kinning, D. J.; Thomas, E. L. *Macromolecules* **1984**, *17*, 1712.
(27) MacKnight, W. J.; McKenna, L. W.; Read, B. E.; Stein, R. S. *J. Phys. Chem.* **1968**, *72*, 1122.
(28) Eisenberg, A.; Navratil, M. *Macromolecules* **1974**, *7*, 90.
(29) Creton, C.; Leibler, L. *J. Polym. Sci., Part B: Polym. Phys.* **1996**, *34*, 545.
(30) Shull, K. R.; Ahn, D.; Chen, W.-L.; Flanigan, C. M.; Crosby, A. J. *Macromol. Chem. Phys.* **1998**, *199*, 489.
(31) Barquins, M.; Maugis, D. *J. Adhes.* **1981**, *13*, 53.
(32) Crosby, A.; Shull, K. R. *J. Polym. Sci., Part B: Polym. Phys.*, in press.
(33) Zosel, A. *Colloid Polym. Sci.* **1985**, *263*, 541.
(34) Lakrout, H.; Sergot, P.; Creton, C. *J. Adhes.* **1999**, *69*, 307.

MA990873H